Proceedings of the International Gas Turbine Congress 2003 Tokyo
November 2-7, 2003

IGTC2003Tokyo TS-075

Enhanced Impingement Heat Transfer: Comparison of Co-flow and Cross-flow with Rib Turbulators

Gordon E. ANDREWS, R.A.A. ABDUL HUSSAIN and Michael C. MKPADI

Energy and Resources Research Institute
Department of Fuel and Energy
The University of Leeds
LEEDS, LS2 9JT, UK
Phone 44 113 2332493, E-mail: g.e.andrews@leeds.ac.uk

ABSTRACT

Impingement flat wall cooling, with 15,2 mm pitch square hole arrays, was investigated in the presence of an array of plain (Type A) and slotted rib (Type B) obstacles. There was one rib for each row of impingement jets. Type B ribs took the form of rectangular pin-fins and both rib forms had a 50% blockage to the crossflow when mounted normal to the crossflow. However, this gives the largest pressure loss and this work compared these two rib configurations with the lower pressure loss situation of the impingement jet outflow parallel to the ribs. The results showed that the increase in surface average impingement heat transfer, relative to that of a smooth wall was small. The main effect of the slotted ribs was to change the influence of crossflow. For a smooth wall crossflow produced a deterioration in the heat transfer with distance. With the slotted ribs the heat transfer increased with distance. The influence of parallel flow relative to crossflow was also small, but for smooth ribs there was a significant improvement in the surface average heat transfer, whereas for the slotted ribs there was a small deterioration.

INTRODUCTION

Impingement cooling is used in gas turbine blade internal cooling for platform and airfoil surfaces in the mid-vane region. Impingement cooling is also used in combustor wall cooling for low NOx gas turbine combustion, where no film cooling is desirable due to the adverse increase in NOx and CO (Andrews and Kim., 2001). The present work set out to investigate a regenerative cooling configuration for combustor cooling applications. The aim of the regenerative cooling is either to use all of the low NOx burner combustion air for wall cooling prior to injection of that air through the low NOx burner or to use impingement cooling of the combustor and then dump the cooling air into the dilution zone. In the former case the impingement cooling system needs to have a low pressure loss at high mass flow rates and in the second system the impingement cooling system can have the full combustor pressure loss of 3-4% across it.

For larger X/D the pressure loss increases and if this is to be kept low then the mass flow rate has to be lower. This then limits high X/D impingement cooling to using only a portion of the combustion air flow and discharging this air through wall film cooling jets in the transition duct or through dilution holes. This is the procedure currently used in most low NOx combustor cooling applications of this technique. In future low NOx combustors all the compressor air will be required for combustion and the use of this type of impingement cooling is likely to be replaced by regenerative cooling with a low pressure loss, small X/D high mass flow design requirement. Hence, the importance of investigating factors that influence the pressure loss. One such factor investigated in this work is the relative direction of the impingement generated crossflow to the ribs.

For turbine vane cooling it is normally the mid-passage and the tip region that is impingement cooled (Son et al., 2001). The mid-vane region has a geometry that can be represented by flat plate impingement heat transfer, sometimes with an upstream crossflow in the impingement gap. This upstream flow is the flow from the tip cooling region, which in many cases is an impingement cooled region. Some recent investigators of enhanced impingement cooling have used experimental configurations with imposed upstream crossflow (Haiping et al., 1997, 1998). However, if the turbine tip area is cooled with impingement air jets, that are subsequently used for tip film cooling then the mid-passage region has no upstream crossflow and some recent investigators of impingement cooling with obstacles in the gap have used this configuration (Hoecker et al., 1999; Annerfeldt, et al., 2001).

Impingement cooling, with several rows of holes with a single direction of discharge flow, self generates a crossflow for the downstream rows of holes from the discharge from the upstream rows. For smooth walls this crossflow results in a decrease in the impingement heat transfer with axial distance (Chance, 1974; Kercher and Tabakoff, 1970; Florschuetz, et al., 1981; Abdul Hussain and Andrews, 1990). However, with obstacles in the gap it is anticipated that their prime effect may be to interact with the crossflow to enhance

Copyright © 2003 by GTSJ
Manuscript Received on September 29, 2003

the heat transfer and hence have the greatest influence on the downstream portion of the test sections. This was first shown by Trabolt and Obot (1987) for small transverse ribs and by Abdul Hussain and Andrews (1991) for large transverse ribs, slotted ribs and ribs with circular holes.

These investigators also showed that the obstacles degraded the impingement heat transfer in the leading edge region, where cross flow was low. This is considered to be due to the ribs preventing the interaction between the impingement jets on the impingement wall surface so that turbulence levels were lower, resulting in lower heat transfer. Overall, the surface averaged impingement heat transfer for the whole surface area was only increased by a small amount and sometimes was decreased, due to these opposing leading and trailing edge effects of obstacles. Similar results were found in the present work.

Combustor wall cooling for low NOx emissions applications usually involves impingement cooled walls with no upstream crossflow. However, with a large number of rows of impingement holes there is a self-generated crossflow experienced by the downstream or trailing edge holes. There are normally more rows of impingement holes than are used in gas turbine blade cooling, as the surface areas are greater. In essence there is little difference between an imposed upstream crossflow and one that results from the discharge of a number of upstream rows of holes, apart from increased turbulence levels in the crossflow. In the present work the downstream area of the test plate with 10 rows of impingement jets, experienced an upstream crossflow from the discharge of the leading edge impingement holes. It will be shown that the greatest influence of the slotted rib roughness elements on the impingement heat transfer was in the downstream area of the test walls, where upstream crossflow was significant.

For both combustor wall and turbine blade cooling the pressure loss of the cooling system is important as this determines coolant mass flow rates. In turbine blades the main pressure loss is usually at the impingement jet holes and the crossflow pressure loss is small, these geometries are characterised by large impingement hole pitch, X, to diameter, D, ratios, X/D (Andrews and Hussain, 1986, 1987). For combustor wall impingement cooling applications the main pressure loss can be at the impingement jets, if the air is to be discharged into the combustor at a low pressure loss transition duct film cooling slot, or as dilution air. In these applications the air mass flow rate is low and the jet pressure loss is high. However, if the impingement backside cooling air is to be used as regenerative cooling prior to discharge as the main low NOx combustor air supply (Andrews et al., 1993) then the impingement wall pressure loss has to be low (small X/D) and the coolant mass flow rate high.

A further problem with impingement cooling and crossflow interactions is that as the impingement wall pressure loss is reduced then the pressure loss due to the crossflow becomes a greater proportion of the overall pressure loss. This can then lead to a flow maldistribution between the rows of impingement holes (Florschuetz et al., 1981). The geometries for which flow maldistribution was important was shown by Andrews and Hussain (1986, 1987) to be predicted by the parameter w in Eq.1, for a constant density between the jet and crossflow. If the jet velocity ratio, U_j / U_c was less then 2 or w less than 6, then flow maldistribution was significant and increased as w decreased or Uj/Uc decreased.

$$w = [U_j /(U_c\ C_d)]^2 = [(1/C_d\ NA)\ Z/D]^2 \quad (1)$$

In the present work with obstacles in the gap the increase in pressure loss due to the crossflow caused by the obstacles will increase the flow maldistribution. However, the effect of flow maldistribution is to divert cooling air from the leading edge to the trailing edge of the impingement cooled gap and this enhances heat transfer in the trailing edge region, but reduces the upstream crossflow. These effects will be shown to be relatively small in the present work.

RIB ENHANCED IMPINGEMENT HEAT TRANSFER LITERATURE REVIEW

In the present work a high rib blockage of the impingement gap of 50% was investigated. This blockage had previously been investigated by Abdul Hussain and Andrews (1991), for three rib designs. Their results showed some of the highest enhancement in impingement heat transfer in the literature. This high crossflow blockage of 50% is larger than has been studied by most other workers. The reason for the significance of large blockage obstacles rather than small boundary layer trip obstacles, is the generation of large-scale recirculation zones in the impingement gap with associated turbulence generation. These aerodynamics are generated by the interaction of the induced crossflow in the downstream portion of the impingement gap with the large obstacles. The review of previous work below shows that the highest enhancements of impingement heat transfer due to obstacles in the gap are for geometries with a high crossflow blockage.

The internal aerodynamics of impingement jet arrays in a closed duct with Z/D less than about 10 were investigated using CFD by Abdul Hussain and Andrews (1991) and Al Dabagh et al. (1989). These CFD studies have been experimentally confirmed in the studies of Son et al (2000, 2001) for triangular impingement hole arrays. The impingement jet flows interact to generate a reverse flow on the centreline between adjacent holes and in the present work the rib was located so that each side of the rib was scrubbed by this reverse flow. The intention was to increase the convective heat transfer with the ribs and also to increase the surface area available for heat transfer (by 79.8%). The action of the crossflow would create additional turbulent wake interactions with the ribs.

It has not previously been recognised that the obstacle blockage to the crossflow is an important parameter in the enhanced heat transfer, as it is rarely given in the papers. The blockages have been evaluated from the geometries given in the papers. Kercher and Tabakoff (1970) studied very narrow gaps with between 11-34% blockage by the ribs. Trabold and Obot (1987) investigated small ribs in large gaps with a blockage range from 1.6 to 12.8% for X/D = 3.15 and 1.78.. Shizuya and Kawaike (1987) investigated a single rib blockage of 12.5% and pin-fin obstacles with blockages of 16% and 40% for an X/D of 4 and 8. Chang et al. (1997, 1998) investigated continuous crossflow ribs with blockages of 25, 38 and 50% in the presence of upstream crossflow and for X/D = 5, 7.5 and 10 with square hole arrays. These geometries would give higher impingement wall pressure loss then in the present work and there would be no significant flow maldistribution. They showed that for the same impingement jet Reynolds number the higher the blockage of the ribs the higher was the Nusselt number and that the influence of the ribs increased as the crossflow velocity increased relative to the impingement jet velocity.

The circular pin-fin obstacle array in the impingement gap used by Hoecker et al. (1999) was of diameter larger than the impingement jet diameter. The pin height to diameter ratio was 1. The blockage used by Hoecker et al. (1999) was

varied by increasing the impingement gap. Blockages of 10, 20 and 30% were investigated for X/D = 4.35, 6.5 and 13. However, the pin fin blockage was not varied as an independent parameter, as X/D was decreased as the blockage was increased and hence the impact of the pin-fin blockage was not determined. For an X/D of 6.5 and a 20% blockage the heat transfer enhancement was between 10 and 35%. For an X/D of 4.35 and a blockage of 30% the effect of the pin fins varied from an enhancement of less than 5% to a deterioration of up to 5%.

The earliest investigation of enhanced impingement heat transfer using pin-fins was by Shizuya and Kawaike (1987) for a constant Z of 8mm and D of 2.5mm. Roughness elements of repeated rectangular ribs, pin-fins, and combinations of ribs and pin-fins were investigated on flat and concave surfaces. Transverse ribs alone, with a blockage of 12.5%, had negligible influence on the heat transfer, but the addition of pin-fins with a blockage of 40% increased the heat transfer by 50% for an X/D of 4 and by 16% for an X/D of 8. This is the highest reported influence of surface roughness on impingement heat transfer and the best geometry had 2 pin-fins for each impingement hole. The results showed that the greatest influence of the pin-fin obstacles was for the highest crossflow blockage, although this was not directly stated. There was no comparison of the various surface roughness elements at constant crossflow blockage, as in the present work.

Annerfeldt et al. (2001) investigated enhanced impingement heat transfer using various pin-fin arrays including round, triangular, 'V' gutter and rectangular pin-fin shapes. The rectangular pin-fin geometry was aligned with the shortest width into the flow, giving the lowest blockage. In the present work the rectangular pin-fins have the longest side into the crossflow, giving the 50% blockage. This geometry was compared with the lower blockage of the ribs parallel to the crossflow, similar to the work of Annerfeldt et al. (2001) The crossflow blockages studied by Annerfeldt et al. (2001) were 13-39% for triangular and 'V' gutter pins, 8-24% for cylindrical pins and 4-14% for rectangular pins. An X/D of 5 was used in the study, similar to the present work X/D of 4.66. The results showed the greatest enhancement of heat transfer for the geometries with the highest blockage, for the same impingement X/D. The maximum enhancement for the triangular pins was 30%.

IMPINGEMENT JET ARRAY AND RIB CONFIGURATIONS

Two impingement target walls were used: one with ten equispaced continuous ribs (Type A) and one with ten slotted ribs (Type B), as shown in Fig.1. Both the ribs were 3mm thick. The rib was not attached to the outer wall to avoid the thermal stresses that would occur in combustor cooling with a hot inner wall and cool outer wall. The impingement crossflow configurations investigated are shown in Fig. 2. The impingement gap, Z, was 9 mm for both ribs and both configurations gave a blockage, when mounted normal to the crossflow, of 50% of the impingement gap (crossflow). When mounted parallel to the crossflow (co-flow) Type A ribs had a blockage of 8.0% and Type B 14.2%, these lower blockages resulted in lower pressure loss for the co-flow configurations.

For the Type B slotted rib there were 10 slots of 6.6 mm width so that there was one rib for each of the 100 impingement holes. This geometry left a flat plate obstacle, 3mm thick, of 8.59 mm width and 8mm height for each impingement jet. The distance from the rear face of rib to the front face of the downstream rib for Type A and B ribs was 12.2mm and this was much bigger than the impingement hole investigated of 3.27 mm diameter. The impingement wall X/D was 4.66 and the Z/D was 2.75.

The surface area of the Type A ribs gave a 59% increase in the heat transfer surface area of the impingement wall, per impingement jet. Type B ribs gave a 79.8% increase. The rib was positioned so that the impingement jet was aligned with the centre line of the flat obstacle and midway between two consecutive obstacles, as shown in Fig.1. Any influence of the increase in surface area for heat transfer due to the ribs was concluded to be part of the effect of the ribs and all heat transfer comparisons was on the basis of the same flat surface area of the smooth impingement target surface.

EXPERIMENTAL TECHNIQUES

The experimental techniques have been fully detailed previously (Abdul Hussain and Andrews, 1990, 1991; Andrews and Hussain, 1984) and shown to have excellent repeatability and to give good agreement with the mean surface averaged heat transfer coefficient measurements using alternative techniques (Chance, 1974, Kercher and Tabakoff, 1970). A 152mm square test section was mounted on the base of an internally insulated plenum chamber for the coolant supply. The impingement gap was made using a stainless steel spacer with a flow discharge from the downstream edge of the gap.

Both the 6.3mm thick stainless steel impingement target plates with roughness elements and the impingement jet plates were instrumented with brazed embedded mineral insulated Type K thermocouples. The thermocouple leads were fed along the surface of the impingement wall on the electrical heater side. This side was well insulated and there was negligible heat losses through the thermocouple leads. Sufficient transverse thermocouples on the centreline were used to establish that the central axial region was not influenced by any side wall effects.

The axial variation of the temperatures along the centre line in the direction of the crossflow of impingement air was determined. The thermocouples were spaced every 15.2mm on the centreline of the target wall mid-way between the centre two rows of impingement jets. These enabled the axial variation of the surface averaged heat transfer coefficient to be determined. Conduction within the test wall gave a locally uniform wall temperature and hence a surface average heat transfer coefficient was determined for each thermocouple location.

The test wall was electrically heated in the absence of any impingement coolant flow to a temperature of approximately 80^{o}C. The electrical power was switched off and the coolant flow initiated at a preset flowrate and the plate temperature monitored as a function of the time. The conductive metal wall is a situation of low Biot number. The transient cooling is governed by a first order response and the time constant, T, was determined from the results.

$$T = m C / hx Ap \qquad (2)$$

Where hx is the local surface averaged heat transfer coefficient at the axial position of the thermocouple.

The mass of the ribs was included in the thermal mass of the wall. The heat transfer surface area, Ap, was taken as the same as that of the smooth wall, ignoring the increase in surface area due to the ribs. This procedure has also been used by other workers investigating the influence of ribs on convective heat transfer (Tabakoff and McFarland, 1975; Han, 1984; Trabold and Obot, 1987). Hoecker et al. (1999) are the only investigators to include the area of the pins in the

impingement heat transfer surface area. The use of the same heat transfer surface area for the smooth and rough surfaces, essentially allows any effect of the increased surface area of the pins to be included in the overall effect of the pins on the heat transfer.

Error analysis shows that the main error in the determination of the heat transfer coefficient is the determination of the time constant in Eq. 2 from the transient temperature data using Type K thermocouples. The time constant was derived as the slope of the line plotting the impingement wall temperature to coolant temperature difference as a function of the rate of change of the wall temperature (Al Dabagh et al., 1989). A least square fit to the line was used. The maximum temperature difference from ambient was 60^{o}C at the start of the cooling process and this was determined with a resolution of 0.1 ^{o}C. The wall temperature to coolant temperature difference was determined with 0.2^{o}C resolution and the accuracy was 0.3% at the start of the cooling and 4% at the end of the cooling when the temperature difference was 5^{o}C.

The rate of temperature change was determined by differentiation of the cooling temperature v. time records for each thermocouple. This then avoids any calibration errors of the thermocouples. The rate of cooling was determined for 5^{o}C temperature drop intervals with a 2% resolution. At least 12 rates of cooling were determined for each thermocouple and these were plotted against the temperature difference. All the data fell within 3% of the best fit line. The coolant mass flow rate was determined using calibrated variable area flow meters too an accuracy of 2% of reading.

The error analysis indicates a maximum possible error of 5% in the time constant and hence in h, when the flow and T errors are combined. Agreement with the results of other workers has been shown to be within 5% for the same geometries. Repeat tests, with a test rig rebuild of the test geometry, have shown that the measurement of h can be repeated to better than 5%.

The range of G investigated was that appropriate for gas turbine combustor wall cooling. A G of 2 kg/s m^2 bar) represents approximately all of the combustor air flow being used to regeneratively impingement cool the combustor wall. Lower values of G represent part of the combustor airflow used for impingement cooling.

PRESSURE LOSS RESULTS

The pressure loss was measured as the static pressure difference between the impingement air supply plenum chamber, upstream of the impingement test wall, and the impingement gap discharge atmospheric pressure. The overall pressure loss was dominated by the pressure loss of the impingement wall. The presence of the smooth impingement wall had little influence on the overall pressure loss for Z/D > 1 (Andrews and Mkpadi, 1983).

The pressure loss results as a function G are shown in Fig. 3. The smooth wall pressure loss was approximately 10% below that for the Type B roughness with crossflow, but greater than the pressure loss for co-flow for both types of roughness. For a coolant flow rate, G, of 1 kg/m^{2}s the smooth wall pressure loss was 0.6 %. The pressure loss with crossflow for Type B roughness was 0.7% and 0.75% with Type A. At the higher flow rates of the order of 2–2.5 kg/m^{2}s, which corresponds to all the combustion air used for cooling, the pressure loss increased to 3-4% for all three wall configurations. This is typical of the combustor wall pressure loss and hence the impingement geometry investigated was of the type where the impingement air was discharged into the dilution zone and not used for combustion.

For the co-flow configuration the pressure loss was found to be less than that for a smooth wall. For Type A roughness the pressure loss for a G of 1 kg/m^{2}s was 0.5%, 20% below that of a smooth wall. A higher flow rates the difference was about 25%. This was an unexpected result and indicates that for a smooth wall the surface interactions between the impingement jets significantly increased the pressure loss. With a wall between the jets this sideways interaction was stopped with a reduction in the turbulence generated and hence in the pressure loss. For the slotted rib B with co-flow the pressure loss was higher than for Type A smooth ribs. The increase in pressure loss from Type A to Type B ribs in co-flow was 16% at high flow rates. The reason for this was the interaction of the co-flow down the channels with the slotted rib wall, which would give higher wall friction pressure loss.

For an X/D of 4.66 with Uj/Uc of 1.8 the flow maldistribution between the leading edge impingement hole and the trailing edge hole can be shown using Eq. 1 to be approximately 24% (Andrews and Hussain, 1986, 1987). For a smooth wall the influence of flow maldistribution is to increase the impingement heat transfer in the trailing edge region, with a decrease in heat transfer coefficient in the trailing edge region in the absence of flow maldistribution (Chance, 1974; Abdul Hussain and Andrews, 1990). In the present work it will be shown that the influence of flow maldistribution was small. For a smooth wall the heat transfer coefficient decreased with axial distance.

THE AXIAL VARIATION OF THE HEAT TRANSFER COEFFICIENT

The axial variation in the heat transfer coefficient, hx, are shown in Figs.4-7 for two coolant flow rates and both types of surface roughness**.** Comparison is made in each Figure of crossflow (across) and co-flow (parallel) with the results for a smooth wall. These results show that for a smooth wall hx decreases with distance, as found in all investigation of impingement heat transfer where flow maldistribution is not large (Andrews and Hussain, 1987). The small increase in hx in the trailing edge region (120mm) was due to the small flow maldistribution (24% determined from the pressure loss).

For Type A (Rough A) surface roughness Figs. 4 and 5 show that the influence of the orientation of the crossflow relative to the ribs was strong. For co-flow (parallel) the impingement heat transfer was similar to that for a smooth wall. At the higher flow rate in Fig. 5 there was a small increase in heat transfer in the trailing edge region. However, for crossflow (across) the axial variation in hx was for a reduction in the leading edge region and an increase in the trailing edge region. The surface averaged results are shown below to be a small reduction in hx with the crossflow orientation. The higher heat transfer with co-flow was also accompanied by a lower pressure loss, as shown in Fig. 3. For a G of 2.5 kg/m^{2}s the pressure loss was 4.2% for crossflow and 2.8% for co-flow, a reduction ion pressure loss by a third.

These results indicate that with co-flow the smooth ribs parallel to the impingement jet outflow behave in a very similar way to that of a smooth wall. The interaction between the jets in the axial direction, which is the cause of the deterioration in heat transfer with distance, must be similar with the ribs orientated in the flow direction. However, with the ribs normal to the crossflow, the interaction between the axial jets is halted by the ribs. This results in little variation of hx with axial distance.

For Type B rectangular pin-fin array, Figs 6 and 7 show that both orientations of the ribs deviate from the smooth wall performance. For co-flow (parallel) hx was lower at the leading edge and similar at the trailing edge. The net effect was that h did not vary much with axial distance at the lower G in Fig. 6. There was a deterioration with axial distance at the higher G in Fig 7, which was lower than for the smooth wall. The crossflow in the parallel channels experienced a higher wall that was interrupted by the gaps in the slotted rib. These gaps would generate crossflow wall turbulence, which resulted in the higher pressure loss shown in Fig.3, compared with the Type A smooth ribs.

For the Type B rectangular pin-fin array with ribs normal to the crossflow, h had the greatest deviation form the smooth wall results. At the leading edge hx was lower and at the trailing edge it was higher than for a smooth wall. The overall effect was of a small increase in h with axial distance. These results demonstrate that the main advantage of the rectangular pin-fin array was in the trailing edge region where the enhancement in hx was 20% for X/D of 4.6. This trailing edge enhancement of hx was partially due to interaction of the cross flow with the pin-fins to create locally higher crossflow velocities offset from the impingement jets and wake turbulence behind the pin-fins. Also the downstream heat transfer was enhanced by the small flow maldistribution caused by the pressure loss of the pin-fin array. Both of these effects would locally increase the convective heat transfer in the trailing edge region.. In the leading edge region the crossflow effects were small and the deterioration in hx relative to a smooth wall was considered to be due to the obstruction of the interaction on the impingement jet flows that would create turbulence on the surface. The flow maldistribution would also contribute to the reduced heat transfer in the leading edge region.

SURFACE AVERAGED HEAT TRANSFER

The influence of the coolant mass flow rate on the surface averaged heat transfer coefficient, h_{av}, is shown in Figs. 8-11. All the local values for hx on the centreline plain of measurements were averaged to determine h_{av}. Figs. 8 and 9 show h_{av} as a function of the mass flow parameter, G. These show that there was very little difference between h_{av} for co-flow and crossflow for both of the rib geometries. However, there was a small but significant effect of the orientation of the crossflow that was different for the two rib geometries. Fig. 8 shows that for Type A continuous smooth ribs co-flow (parallel) resulted in higher values of the heat transfer coefficient and a steeper dependence on the mass flow rate. Fig. 9 shows that the opposite occurred for the slotted rib or rectangular pin-fin array.

The exponent y for $h_{av} = \text{const}\ G^{y}$, is the same as that for a Nu v. Re plot, as the variable is the coolant mass flow rate. These exponents were evaluated for the higher values of G above 0.6, where there was no change in the dependence of h_{av} on G. At low G the impingement jet Re. was in the turbulent/laminar transition region and hence had a lower dependence of h_{av} on G. For the X/D of 4.66 used in the present work the smooth wall had a value of y of 0.7 and with continuous Type A ribs with co-flow y was 0.86 and 0.84 for crossflow . For the pin fin ribs the value of y was it was 0.79 for co-flow and 0.81 for crossflow. Both types of rib had a significantly greater dependence on flow rate compared with a smooth wall. This was considered to be due to the influence of the interaction between the crossflow in the impingement gap and the ribs.

The results for h_{av} are compared with those for a smooth wall in Figs 10 and 11, where h_{av} for each rib is shown as a ratio to the smooth wall value for both co-flow and crossflow. The results show that in general the action of the ribs investigated for impingement heat transfer was to reduce the surface averaged heat transfer. Only at high G with co-flow was the heat transfer increased for Type A smooth ribs. For Type B pin-fin ribs the surface averaged effect was entirely negative at all values of G investigated.

These results illustrate different trends for the orientation of the flow relative to the ribs. For the smooth ribs co-flow gives of the order of 10% higher heat transfer compared with crossflow. For Type B pin-fin ribs the effect is reversed and crossflow gives higher heat transfer than co-flow. It is considered that the reason for these differences is that with plain ribs and co-flow there is a beneficial influence of the increased rib surface area, which is continuously in contact with the co-flow. Secondary flows normal to the co-flow are also likely to be set up, similar to those in rectangular channel flow. For the slotted ribs co-flow would have interrupted contact with the enhanced heat transfer surface and it is unlikely that secondary flow would be set up. Turbulence levels would be higher with crossflow for pin-fin ribs, resulting in the higher heat transfer. However, the inferior results compared with a smooth wall show that the turbulence created by the impingement jet surface wall jet impingement interactions was significantly greater than that created by crossflow/rib interactions. The presence of the ribs stopped the impingement jet wall flow interactions and the associated turbulence generation.

CONCLUSIONS

The present results show that obstacles of the pin-fin type are only worth using in situations where there is significant crossflow. This may be self-generated crossflow in impingement cooling with many rows of holes and a flow exit in a single direction or it may be the outflow of cooling air from, say, vane tip cooling. In the leading edge region in the absence of crossflow, obstacles degrade impingement heat transfer due to removing aerodynamic interactions between the impingement surface jets.

In the absence of crossflow in the leading edge region heat transfer deteriorates if rectangular pin-fin obstacles are used. This is postulated to be due to reduced surface turbulence caused by the rectangular pins preventing the aerodynamic interaction of the surface jets from adjacent impingement holes.

The direction of the crossflow relative to rib turbulators was expected to have a large influence on the heat transfer. Enhanced heat transfer using ribs is normally investigated using ribs transfer to the crossflow. In the present work it was found that for impingement cooling with smooth (Type A) ribs better heat transfer was achieved for co-flow. This was considered to be due to the benefit of the additional rib surface area and the generation of secondary flows in the channels between the ribs. For slotted ribs the additional turbulence created by crossflow interactions with the rectangular pin-fins gave higher heat transfer than for co-flow. However, none of the four rib configuration investigated had higher surface averaged heat transfer than for a smooth wall.

The main effect of the ribs was to alter the axial dependence of the heat transfer on the crossflow. This was most pronounced for Type B pin-fin ribs in crossflow, where the trailing edge region of the test wall had significantly enhanced heat transfer compared with a smooth wall. In the leading edge region the heat transfer was reduced, due to the reasons discussed above.

The addition of surface area by the use of large pin-fin obstacles was not a significant feature in the enhancement of

the heat transfer. The main influence of the pins was to interact with the crossflow to generate locally higher surface crossflow velocities and turbulence in the wake region behind the rectangular pins. If the surface area increase was significant then this would result in increased heat transfer in the leading edge region, where cross flow is zero.

ACKNOWLEDGEMENTS

We would like to thank the EPSRC for a research grant that provided the equipment used. We would like to thank the Iraq Government for a research scholarship to R.A.A. Abdul Husain. The test facility was construction, commissioned and operated by R.A. Boreham.

REFERENCES

Abdul Hussain, R.A.A. and Andrews, G.E., 1990, 'Full coverage impingement heat transfer at high temperatures'. ASME Paper 90-GT-285.

Abdul Hussain, R.A.A. and Andrews, G.E., 1991, 'Enhanced full coverage impingement heat transfer with obstacles in the gap, ASME Paper 91-GT-346.

Al Dabagh, A.M., Andrews, G.E., Abdul Husain, R.A.A., Husain, C.I., Nazari, A. and Wu, J., Impingement/effusion cooling: the influence of the number of impingement holes and pressure loss on the heat transfer coefficient, ASME 89-GT-188, Also Trans ASME 1989.

Andrews, G.E., Al Dabagh, A.M., Asere, A.AA., Bazdidi-Tehrani, F., Mkpadi, M.C. and Nazari, A. 1992. Impingement/Effusion Cooling. AGARD CP 527, Heat Transfer and Cooling in Gas Turbines, Antalya,Turkey pp. 30-1 – 30-10.

Andrews. G.E. and Kim, M.N. 2001. The influence of film cooling on emission for a low NOx radial swirler gas turbine combustor, ASME Paper 2001-GT-0071.

Andrews, G.E., Asere, A.A., Hussain, C.I. and Mkpadi, M.C., 1985. Full coverage impingement heat transfer: the variation in pitch to diameter ratio at constant gap, AGARD CP 390, Heat Transfer and Cooling in Gas Turbines. Paper 26, pp. 26-1 to 26-13.

Andrews, G.E. and Hussain, C.I., 1984, Full coverage impingement heat transfer: the influence of impingement jet size, 1st UK National Heat Transfer Conference, IChemE Symp. Ser. No. 86 pp. 1115-1124.

Andrews, G.E. and Hussain, C.I., 1986, 'Full coverage impingement heat transfer: the influence of channel height'. 8th Int. Heat Transfer Conference, Hemisphere Pub. Corp., pp. 1205-1211.

Andrews, G.E. and Hussain, C.I., 1987. 'Full coverage impingement heat transfer: the influence of crossflow', AIAA Paper 87-2010.

Andrews, G.E. And Mkpadi, M.C., 1983, Full coverage discrete hole wall cooling: discharge coefficients. ASME Paper 83-GT-79. Also Trans.ASME,J. Turbomachinery, 1983.

Annerfeldt, M.O.., Persson, J.L. and Torisson, T., 2001, 'Experimental investigation of impingement cooling with turbulators or surface enlarging elements'. ASME Paper 2001-GT-149.

Bailey, J.C. and Bunker, R.S., 2002, Local heat transfer and flow distributions for impinging jet arrays of dense and sparse extent. ASME Paper GT-2002-30473,

Chance, J.T., 1974, 'Experimental investigations of air impingement heat transfer under an array of thermal jets'. Tappi, Vol.57, pp.108-112.

Chang Haiping, Jingyu, Z. and Taiping, H., 1998. Experimental investigation on impingement heat transfer from rib roughened surface within arrays of circular jet: Effect of geometric parameters. ASME Paper 98-GT-208.

Florschuetz, L.W., Truman, C.R. and Metzger, D.E., 1981, 'Streamwise flow and heat transfer distribution for jet array impingement with initial crossflow'. Trans ASME, J. Heat Transfer, Vol. 103, pp.337-342.

Haiping, C., Dalin, Z. and Taiping H., 1997, 'Impingement heat transfer from rib roughened surface within arrays of circular jets: the effect of the relative position of the jet hole to the ribs', ASME Paper 97-GT-331.

Haiping, C., Jingyu, Z., Taipping, H., 1998. 'Experimental investigation on impingement heat transfer from rib roughened surface within arrays of circular jets: effect of geometric parameters, ASME Paper 98-GT-208.

Han, J.C., 1984, Heat transfer and friction in channels with two opposite rib-roughened walls, Trans. ASME, J. Heat Transfer, Vol.106, pp.774-781, 1984.

Hoecker, R., Johnson, B.V., Hausladen, J., Rothbrust, M. and Weigand, B., 1999, 'Impingement cooling experiments with flat and pin plate target surfaces'. ASME Paper 99-GT-252.

Kercher, D.M. and Tabakoff, W., 1970, 'Heat transfer by a square array of round air jets impinging perpendicular to a flat surface'. Trans, ASME, J. Eng. Power, pp.73-82.

Shizuya, M. and Kawaike, K., 1987, Experimental investigation of blade internal cooling methods using ribs and fins, Tokyo International Gas Turbine Congress, Paper 87-Tokyo-IGTC-65, Vol. III pp. 159-166.

Son, C.M., Gillespie, D.R.H., Ireland,P.T. and Dailey, G.M., 2000, Heat transfer and flow characteristics of an engine representative impingement cooling system, ASME Paper 2000-GT-219, Also Trans. ASME, J. Turbomachinery, Jan. 2001.

Son, C, Gillespie, D., Ireland, P. and Dailey,G.M., 2001. 'Heat transfer characteristics of an impingement plate used in a turbine vane cooling system', ASME Paper 2001-GT-154.

Tabakoff, W. and McFarlane, E.R., 1975. Gas turbine blade heat transfer with rough surfaces, ASME Paper 75-WA/HT-107.

Trabold, T.A. and Obot, N.T., 1987, 'Impingement heat transfer within arrays of circular jets. Part II: Effects of crossflow in the presence of roughness elements'. ASME Paper 87-GT-200.

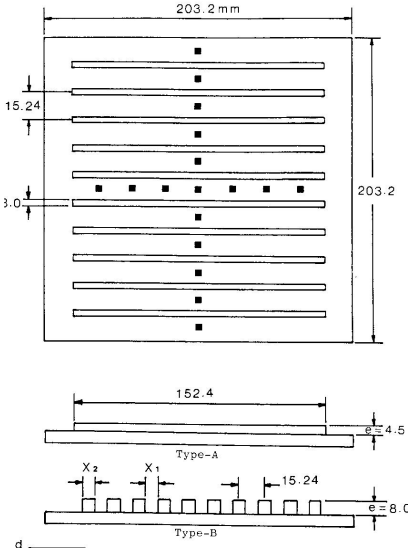

Fig.1 Type A and B ribs and thermocouple locations.

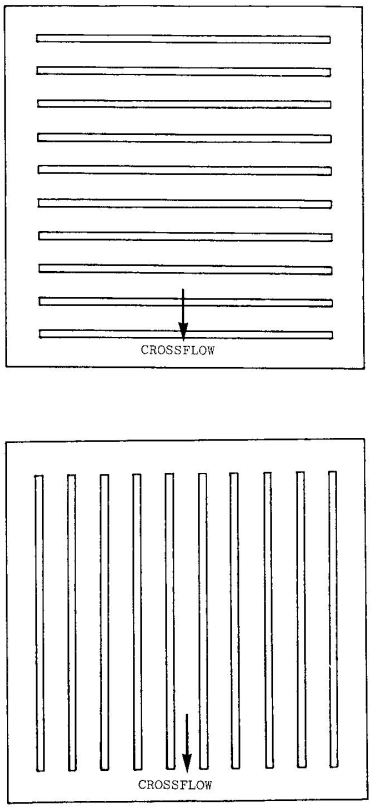

Fig.2
Crossflow (top) and co-flow (bottom) orientation of the ribs relative to the impingement crossflow.

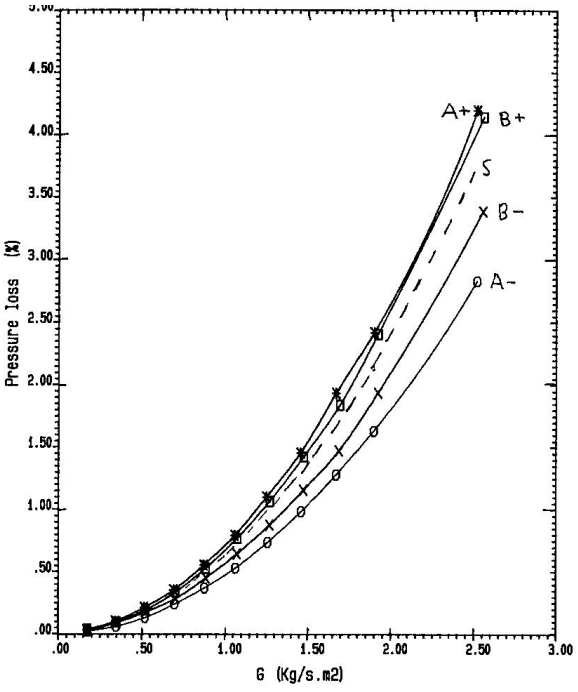

Fig. 3 Pressure loss as a function of the mass flow rate per unit impingement surface area. A+ = Type A ribs with crossflow; A- = Type A ribs with co-flow; B+ = type B ribs with crossflow; B- = Type B ribs with co-flow; S = smooth wall with no ribs.

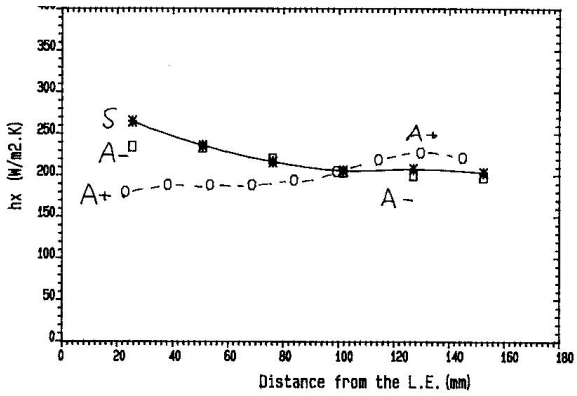

Fig. 4 Axial variation of the local mean average heat transfer coefficient for a G of 0.88 kg/sm^2. Type A ribs, comparison of crossflow and co-flow orientation of the ribs with the smooth wall results. A+ = Type A ribs with crossflow; A- = Type A ribs with co-flow; S = smooth wall with no ribs.

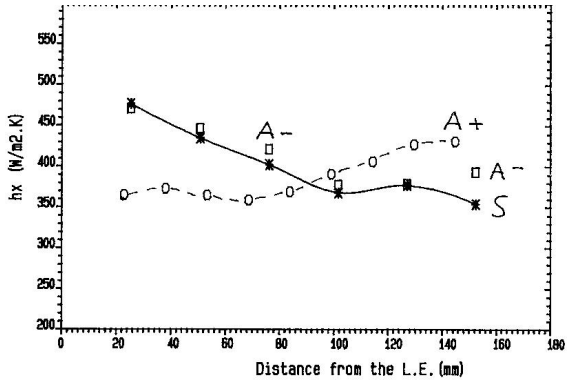

Fig. 5 Axial variation of the local mean average heat transfer coefficient for a G of 1.90 kg/sm^2. Type A ribs, comparison of crossflow and co-flow orientation of the ribs with the smooth wall results. A+ = Type A ribs with crossflow; A- = Type A ribs with co-flow; S = smooth wall with no ribs.

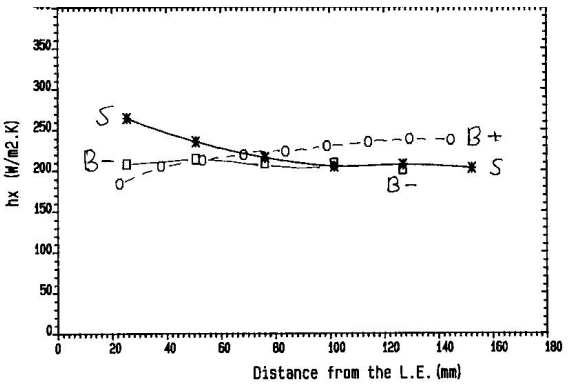

Fig. 6 Axial variation of the local mean average heat transfer coefficient for a G of 0.88 kg/sm^2. Type B ribs, comparison of crossflow and co-flow orientation of the ribs with the smooth wall results. B+ = type B ribs with crossflow; B- = Type B ribs with co-flow; S = smooth wall with no ribs.

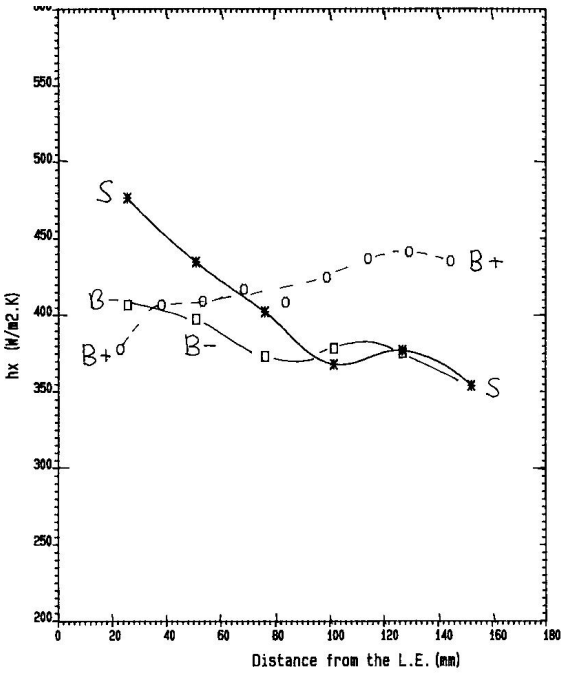

Fig. 7 Axial variation of the local mean average heat transfer coefficient for a G of 1.9 kg/sm^2. Type B ribs, comparison of crossflow and co-flow orientation of the ribs with the smooth wall results. B+ = type B ribs with crossflow; B- = Type B ribs with co-flow; S = smooth wall with no ribs.

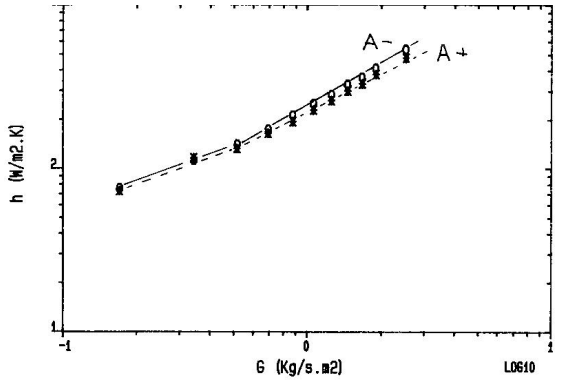

Fig. 8 Surface averaged heat transfer coefficient as a function of the impingement mass flow parameter G for Type A ribs. Comparison of crossflow and co-flow impingement outflow direction relative to the ribs. A+ = Type A ribs with crossflow; A- = Type A ribs with co-flow.

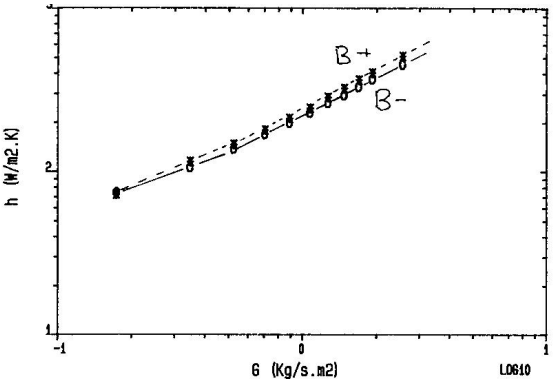

Fig. 9 Surface averaged heat transfer coefficient as a function of the impingement mass flow parameter G for Type B ribs. Comparison of crossflow and co-flow impingement outflow direction relative to the ribs. B+ = type B ribs with crossflow; B- = Type B ribs with co-flow.

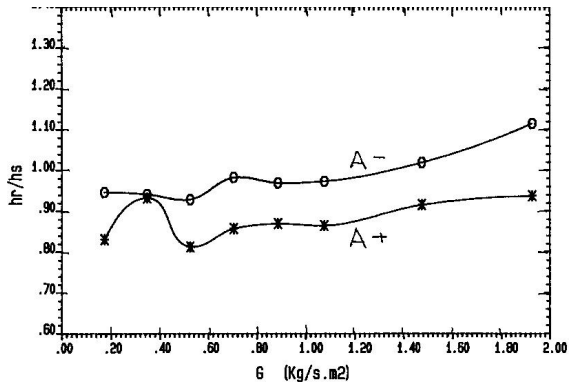

Fig. 10 Surface averaged heat transfer coefficient as a function of the impingement mass flow parameter G for Type A ribs. Ratio of crossflow and co-flow surface averaged heat transfer coefficient to that for a smooth wall. Impingement X/D = 4.66, Z/D=2.75. A+ = Type A ribs with crossflow; A- = Type A ribs with co-flow.

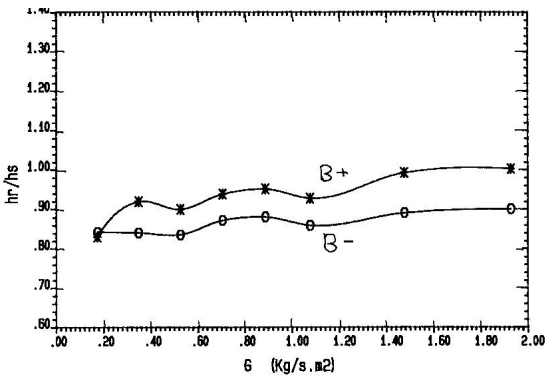

Fig. 11 Surface averaged heat transfer coefficient as a function of the impingement mass flow parameter G for Type B ribs. Ratio of crossflow and co-flow surface averaged heat transfer coefficient to that for a smooth wall. Impingement X/D = 4.66, Z/D=2.75. B+ = type B ribs with crossflow; B- = Type B ribs with co-flow.